Progress In Electromagnetics Research Letters, Vol. 108, 65–73, 2023

Landslide Area Identification and Detection Method Based on Micro-Variation Monitoring Radar Images

Shaoshuai Zhang[1, 2], Yaolong Qi[1, 2, *], Pingping Huang[1, 2], Weixian Tan[1, 2], and Yuejuan Chen[1, 2]

Abstract—Micro-variation monitoring radar based on the differential interference principle can monitor objects prone to micro deformation. However, it is easily affected by human and environmental factors to cause the radar image to loss coherence in the long-term monitoring work, thus affecting the normal monitoring of radar. Therefore, it is of great significance to study the change detection method of micro-variation monitoring radar images, which can provide reference information and quantitative analysis for monitoring work. In this paper, a method of landslide area identification and detection based on micro-variation radar image is proposed. Based on the radar coherence coefficient image of time series, the difference image is produced by logarithmic ratio cumulation. The difference map is decomposed and denoised by wavelet transform, and then the final difference map is produced by reconstructing the processed wavelet coefficients. Finally, the improved K-means is used to cluster the difference map to get the change detection result image. The actual monitoring data of a mining area is used for variation detection. The results show that the proposed method retains the detailed information of the change area and removes a lot of noise. The difference map is easier to cluster, and the clustering result is more accurate.

1. INTRODUCTION

China is rich in mineral resources. With the continuous expansion of open-pit mining, geological disasters occur frequently which seriously threaten the safety of people's lives and property, especially landslide disasters. The detection and analysis of changes in disaster areas are of great significance to safety production. Micro-variation monitoring radar can monitor objects that are prone to micro-deformation through the principle of interferometry. At present, it has been widely used for the monitoring and early warning of geological disasters. However, in long-term monitoring work, due to the influence of human and meteorological factors, radar images in the monitoring area are prone to appear decoherent which affects the long-term monitoring and early warning of radar. Compared with synthetic aperture radar (SAR) image change detection, the research on micro-variation monitoring radar image change detection is much less. The research on fast and effective change detection methods for the incoherent area of the micro-variation monitoring radar image provides important and reliable terrain change information and a supplementary method for long-term quantitative monitoring for the application of the micro-variation monitoring radar in geological disaster monitoring. Therefore, it is of profound significance to deeply study the image change detection method of micro-variation monitoring radar. Take into account this, this paper proposes a landslide region recognition and detection method based on micro-variation monitoring radar images.

Received 11 October 2022, Accepted 14 December 2022, Scheduled 22 December 2022
* Corresponding author: Yaolong Qi (qiyaolong@imut.edu.cn).
[1] College of Information Engineering, Inner Mongolia University of Technology, Hohhot, China. [2] Inner Mongolia Key Laboratory of Radar Technology and Application, Hohhot, China.

Image change detection technology is generally divided into two categories: supervised and unsupervised. Supervised change detection usually requires accurate prior information, while unsupervised change detection [1] algorithm does not need accurate prior information. A considerable amount of coherent speckle noise is usually attached to the image of the micro-variation monitoring radar, which makes it difficult to obtain prior information. Therefore, unsupervised method is more suitable for the change detection task of micro-variation monitoring radar. Ren et al. proposed an unsupervised change detection algorithm based on ground radar images and obtained effective change detection results [2]. The difference map is usually obtained by difference method, ratio method, logarithm method, etc. The difference map obtained by traditional difference method is very sensitive to noise and is not suitable for change detection of micro-variation monitoring radar image. Although the ratio method can effectively suppress speckle noise, it does not consider the local, edge, class conditional distribution, and additional prior information of the image. [3] proposed a SAR image change detection method based on space-time adaptive neighborhood ratio. The coherence coefficient is a measure of the similarity between two variables. Through the coherence coefficient, the similarity between images can be compared, and the changed and unchanged types of images can be preliminarily distinguished. Zhang et al. used the difference method and coherence coefficient of SAR to detect urban changes [4]. There is a lot of speckle noise in the image of micro-variable surveillance radar, which affects the calculation of the coherence coefficient. The logarithmic ratio method [5] converts the multiplicative noise into additive noise, and the difference image has a nonlinear reception and enhances the contrast between the changed and unchanged classes. However, because of the strong contraction of the logarithmic operation, the pixel value in the edge area is easy to be blurred. [6] proposes a method of SAR image change detection threshold based on logarithmic average and gets a better change detection result. The change detection method proposed in this paper can suppress the noise and retain the details of the change area better.

The structure of the paper is arranged as follows. Second 2 introduces the proposed change detection algorithm. Section 3 is the experimental results and analysis of change detection, and Section 4 summarizes the full text.

2. PROPOSED CHANGE DETECTION TECHNIQUE

Time-series micro-variation monitoring radar images are obtained at different times in the same geographical area. The purpose of the radar image change detection for micro-variation monitoring is to detect the changing part of the radar image at different times and generate a binary difference image. The method mainly includes three steps: 1) obtain the coherence coefficient image and perform the logarithmic ratio accumulation operation to generate a difference image with strong contrast; 2) the wavelet decomposes the difference image to obtain the low frequency and high frequency components and performs soft threshold denoising on the high frequency, and reconstructs the coefficients to obtain the final difference image; 3) change detection results using improved K-means cluster difference image. The algorithm flowchart is shown in Figure 1.

2.1. Based on Grouped Time Series Coherence Coefficient Logarithm Ratio Difference Image

The coherence coefficient is used to measure the similarity between two variables. It can measure the similarity of two radar images:

$$R_{tn} = \frac{Cov(I_{n-1}(i,j), I_n(i,j))}{\sqrt{Var\left[I_{n-1}(i,j)\right] Var\left[I_n(i,j)\right]}} \tag{1}$$

where $I_{n-1}(i,j)$ and $I_n(i,j)$ are the time-series adjacent micro-variation monitoring radar images after registration filtering. The value of the coherence coefficient R_{tn} is between 0 and 1. 0 means complete decoherence, and 1 means complete coherence.

The logarithmic ratio operator can convert the multiplicative speckle noise of radar images into additive noise, which is convenient for effectively eliminating speckle noise. The operational formula is:

$$\mathrm{Log}_n(i,j) = \mathrm{Log}\left(\frac{I_{n-1}(i,j)}{I_n(i,j)}\right) \tag{2}$$

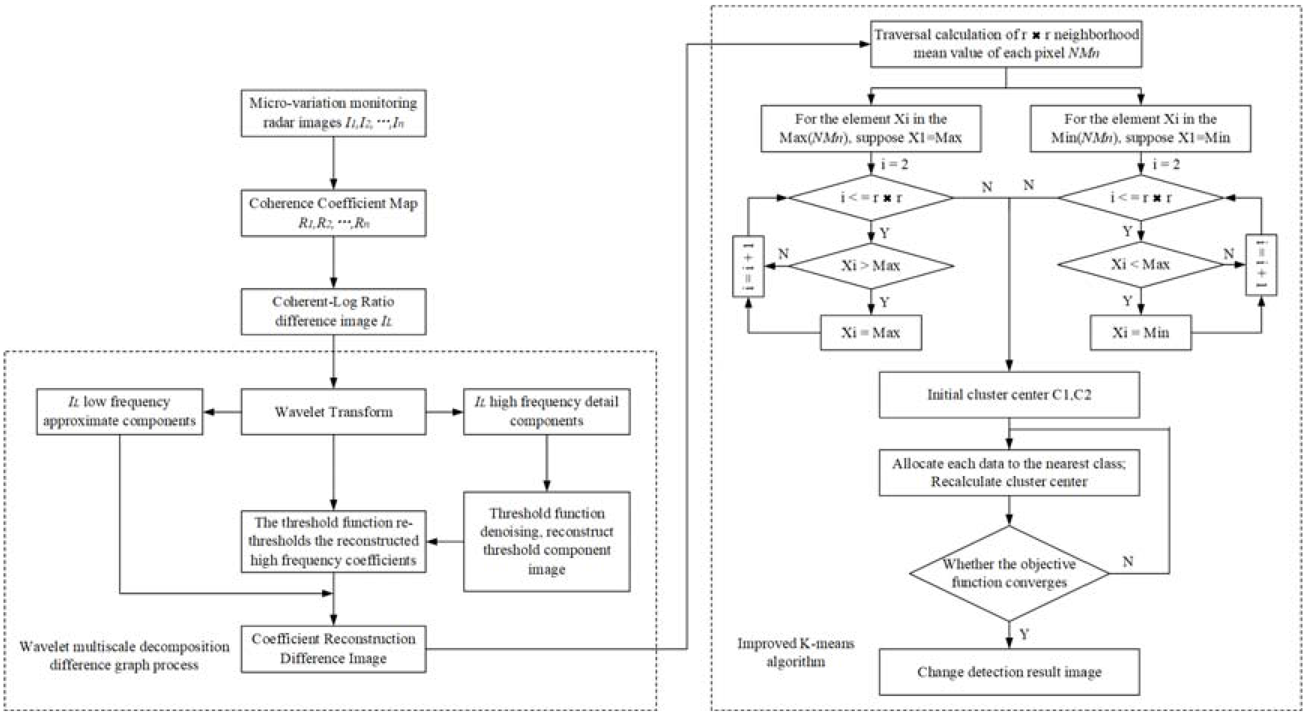

Figure 1. Change detection flowchart.

where $\text{Log}_n(i, j)$ is the log ratio difference image at the n time.

Based on the problem that both the single coherence coefficient difference map and the log ratio difference map are affected by noise and cannot obtain better change detection result, this paper proposes a coherent log ratio difference map algorithm based on time series grouping.

The coherence coefficient of the deformed landslide mass will have a smooth trend of gradually decreasing on the time axis. And the coherence coefficient will decrease in turn, which is expressed as: $R_{t1} > R_{t2} > \ldots > R_{tn}$ & $0 < R_{t1}, R_{t2}, \ldots, R_{tn} < 1$. Then the coherence coefficient of the undeformed landslide mass is expressed as: $R'_{t1} = R'_{t2} = \ldots = R'_{tn}$. On the basis of grouped time series coherence coefficients, the logarithmic ratio difference graph is taken for the accumulation operation as follows:

$$RL_{add1} = \log \frac{R'_{t_2}}{R'_{t_1}} + \log \frac{R'_{t_3}}{R'_{t_2}} + \ldots + \log \frac{R'_{t_n}}{R'_{t_{n-1}}} + \sigma \tag{3}$$

$$RL_{add2} = \log \frac{R_{t_2}}{R_{t_1}} + \log \frac{R_{t_3}}{R_{t_2}} + \ldots + \log \frac{R_{t_n}}{R_{t_{n-1}}} + \sigma \tag{4}$$

where RL_{add1} and RL_{add2} are the value of the undeformed landslide mass and the value of the deformed landslide mass, respectively, and σ is the noise value.

After the calculation, the contrast of the difference image is enhanced, and the value of the landslide area is stretched and increased, while the value of the coherence coefficient for the unchanged area and the noise is between 0 and 1. At this time, the landslide area belongs to the low frequency signal component in the time sequence difference image, while the unchanged area is equivalent to the high frequency signal component of the image. Then the difference map can be decomposed and denoised by wavelet transform.

2.2. Wavelet Analysis Difference Image

The boundary of the landslide area is concentrated in the high frequency part of the image, while the whole area belongs to the low frequency part of the image on the time axis. Therefore, the analysis of the difference map needs to be able to extract and analyze the low frequency part and also to denoise the high-frequency part. Wavelet transform has good local time-frequency analysis ability which can meet the analysis of low frequency and high frequency parts of the difference map from the perspective of multi-resolution [7] and can realize the effective separation of the landslide area and noise.

2.2.1. Wavelet Multiresolution Analysis

Wavelet multi-resolution analysis is to perform multi-layer decomposition on the difference image and then decompose the low frequency components obtained in the previous layer into low frequency components and high frequency components in turn until the required number of decomposition layers is obtained. The decomposition process is shown in Figure 2. The n-layer decomposition is expressed as follows:

$$f(I_c(x,y)) = CA_n + CD_n + CD_{n-1} + \ldots + CD_2 + CD_1 \tag{5}$$

where $I_c(x,y)$ is the difference image, CA_n the low frequency approximation part, CD_n the high frequency detail part, and n the number of layers.

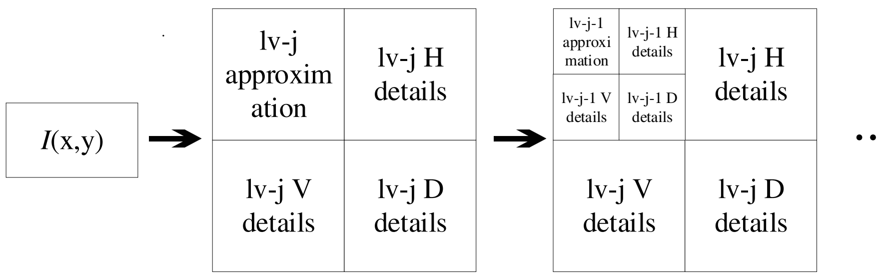

Figure 2. Wavelet decomposition diagram.

2.2.2. Denoising and Reconstruction Process

The difference map and noise have different characteristics after wavelet transformation. The absolute value of the wavelet coefficient of the original difference map information is larger, while the absolute value of the wavelet coefficient of the noise information is smaller. The soft threshold function is selected to compare the wavelet coefficient of the noise signal to the selected threshold value [8]. The point greater than the threshold shrinks to the difference between the point value and the threshold; the point less than the opposite number of the threshold shrinks to the sum of the point value and the threshold; and the point whose absolute value is less than or equal to the threshold is 0. The mathematical expression is as follows:

$$T_{soft} = \begin{cases} 0 & (|y| < T) \\ \mathrm{sgn}(y)(|y| - T) & (|y| \geq T) \end{cases} \tag{6}$$

where y is the noise-containing wavelet coefficient of variation. T is the denoising threshold, and $\mathrm{sgn}(y)$ is a symbolic function.

2.2.3. Improved K-Means Clustering

K-means clusters data into different clusters according to Euclidean distance $d(x_i,\, c_j)$ [9]. The formula for calculating the distance from each data in the difference map to the cluster center is as follows:

$$d(x_i, c_j) = \sqrt{(x_i - c_j)^2} \tag{7}$$

where $x_i (i = 1, 2, \ldots, n)$ represents the data points belonging to cluster j, and the cluster center point $c_j (i = 1, 2, \ldots, k)$ represents the average value of the data in the data set cluster j.

The goal of K-means is to minimize the sum of squares of the distance between each cluster member and its cluster center, so as to obtain the best clustering result [10]. The objective function is:

$$\arg_c \min j(c) = \arg_c \min \sum_{j=1}^{k} \|x - c_j\|_2^2 \tag{8}$$

where c is the set of cluster centers.

The initial cluster centers randomly selected by traditional k-means may increase the number of iterations and increase the amount of computation, and different cluster centers often have different results. In this paper, according to the characteristics of the landslide mass in the difference map of micro-variation monitoring radar is concentrated in this area, and the data value is higher than the unchanged area in the difference map and the noise. The selection rule of the initial cluster center is improved to reduce the influence of random selection on the clustering effect.

The improved K-means calculation process is as follows:

- With each pixel as the center and take a $r \times r$ window to traverse the image to obtain the average value of the neighborhood NM_n. The expression is as follows:

$$NM_n = \frac{1}{r^2} \sum_{x_i \in Nr_n} \sum_{i=1}^{r^2} |x_i| \tag{9}$$

- Compare and sort the neighborhood mean obtained in (9), find the neighborhood of the maximum value and the minimum value. Then sort all the data points in the neighborhood, respectively. Finally, take the maximum data value in $Max(NM_n)$ and the minimum data value in $Min(NM_n)$ as the initial cluster center point of the two classes, respectively.

$$c_1(1) = \mathrm{Max}(\mathrm{Max}(NM_n)) \tag{10}$$

$$c_2(1) = \mathrm{Min}(\mathrm{Min}(NM_n)) \tag{11}$$

- Calculate the distance from each data point to the cluster center point, and assign each data point to the cluster corresponding to the k cluster centers according to the minimum distance principle:

$$\min\left\{\left\|x - c_i(n)\right\|, i = 1, 2, \ldots, k\right\} = \left\|x - c_i(n)\right\|, x \in S_j(n) \tag{12}$$

where n is the iterative operation sequence number.

- Recalculate the average of all data in each cluster as the new center point of the cluster:

$$c_j(n+1) = \frac{1}{N_j} \sum_{x \in S_j(n)} x, j = 1, 2, \ldots, k \tag{13}$$

Steps (12) and (13) are repeated until the cluster center point is basically unchanged, or the criterion function converges to the set threshold, and the algorithm ends. Finally, use (14) to binarize the two cluster sums $S_1(n)$ and $S_2(n)$ which belong to the final cluster centers $c_1(n)$ and $c_2(n)$ calculated by n iterations of the algorithm to obtain the final change detection result map.

$$\mathrm{Img}_{\_change} = \begin{cases} 1 & c_1(n+1) \in S_1(n) \\ 0 & c_2(n+1) \in S_2(n) \end{cases} \tag{14}$$

where $S_1(n)$ is the change class, and $S_2(n)$ is the unchanged class.

3. EXPERIMENT AND ANALYSIS

An experimental study was carried out using the ground imaging radar (LSA) image data from an open-pit mine in China. During the micro-variation monitoring radar monitoring period, a slope landslide occurred at the construction site. Figure 3 is the radar slice image before the landslide, and the data collection time is April 18, 2021. Figure 4 is the radar slice image after the landslide, and the data collection time is April 21, 2021.

Figure 5 shows the coherence coefficient diagram obtained from the experimental data in Figure 3 and Figure 4. Figure 6 is the difference diagram of coherent logarithmic ratio obtained by using

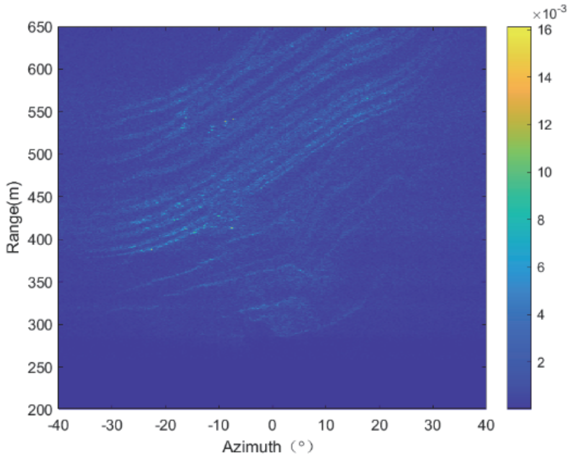

Figure 3. Slice data before landslide.

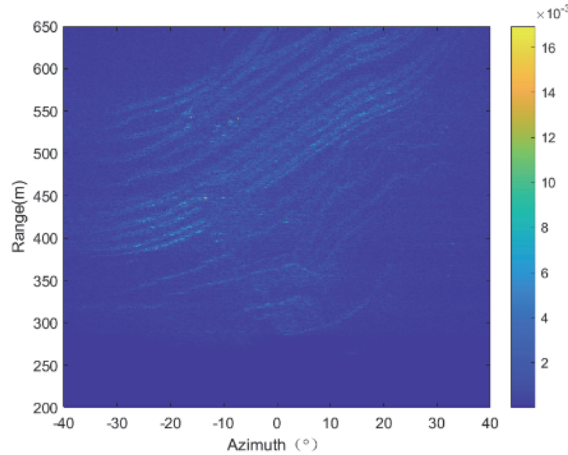

Figure 4. Slice data after landslide.

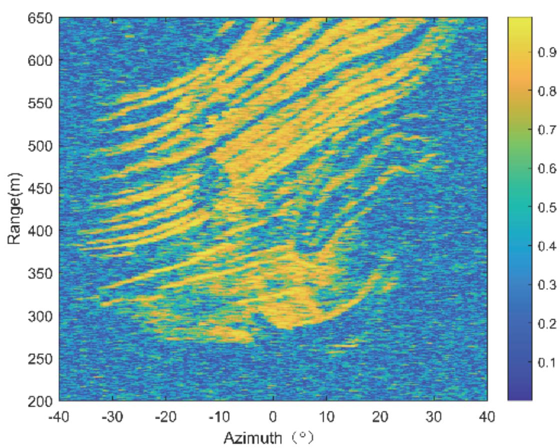

Figure 5. Coherence coefficient map.

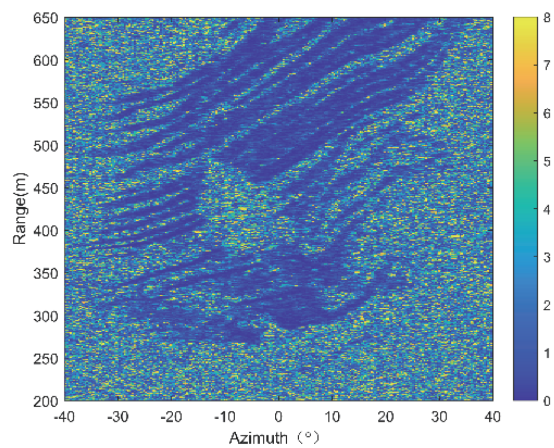

Figure 6. Coherent-Log Ratio map.

logarithmic ratio operator on the basis of coherent coefficient. It can be seen that the difference map contains a lot of decoherent areas caused by speckle noise, and it is difficult to identify landslide areas. After accumulating the difference diagram of the coherent logarithmic ratio of the time series, the contrast between the change class and the unchanged class can be enhanced. As shown in Figure 7, the value of the landslide area RL_{add2} can be stretched, while the value of the unchanged area RL_{add1} is mostly close to 0, resulting in a contrast-enhanced difference map.

The difference map obtained by wavelet threshold denoising is shown in Figure 8. Compared with Figure 5 and Figure 6, it can be clearly seen that the difference map obtained in this paper enhances the contrast between the landslide area and the unchanged area and suppresses the noise well, reducing the impact of noise on the clustering results. In addition, the contour of the landslide area remains intact, and the difference map can be more easily clustered.

To detect the change of the radar image of the micro-variation monitoring, this paper obtains the difference map according to the characteristics of the change of the coherence coefficient of the landslide area in the time series and improves the K-means rule for selecting the initial clustering center. Finally, the improved clustering effect is compared with the traditional K-means algorithm and K-means++ algorithm. The results are shown in Figure 9, Figure10, and Figure 11. Figure 9 is the traditional K-means clustering result, and Figure 10 is the K-means++ clustering result. Figure 11 is the change detection result obtained by the improved K-means in this paper, where the blue pixel value is 0 to indicate the unchanged area, and the yellow pixel value is 1 indicates a change area.

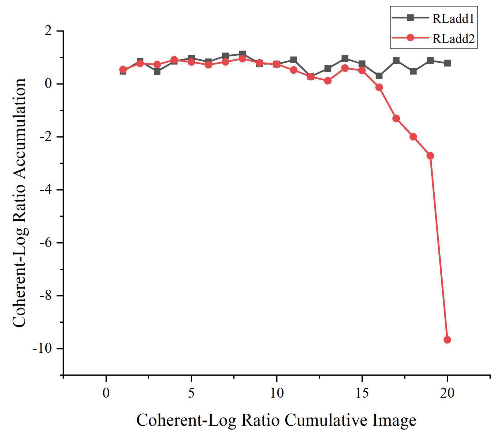

Figure 7. Time series accumulation result graph.

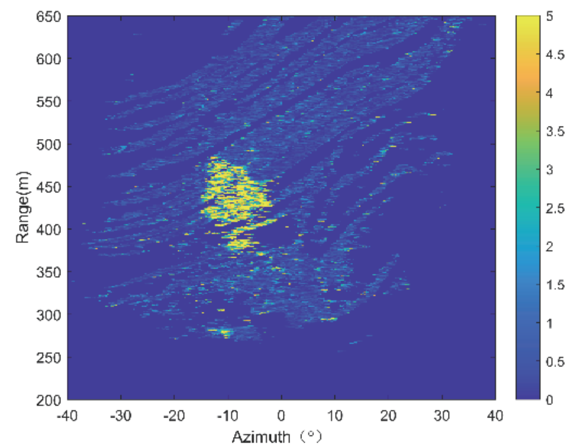

Figure 8. Time series accumulation result map.

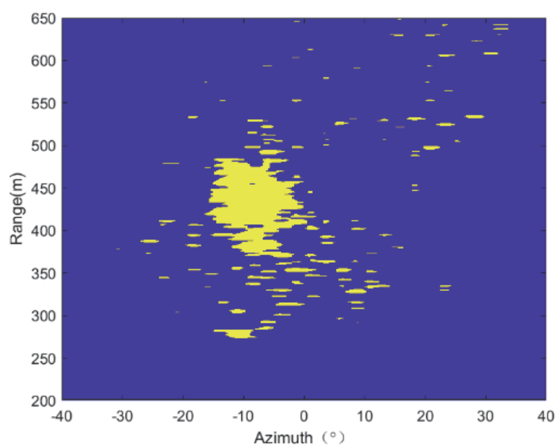

Figure 9. K-means clustering result.

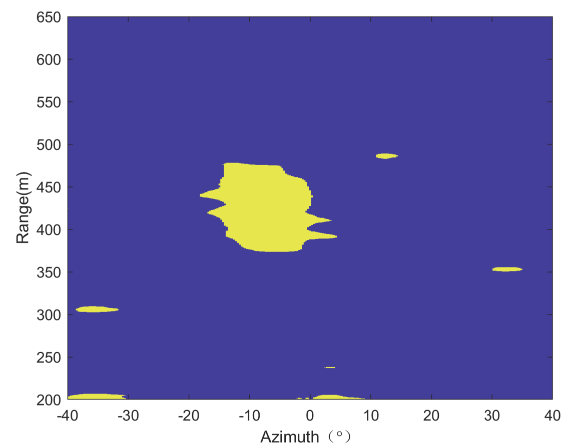

Figure 10. K-means++ clustering result.

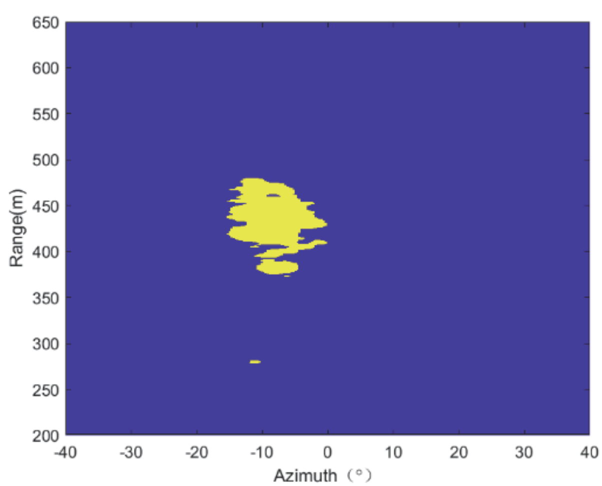

Figure 11. Improved K-means clustering result.

It can be clearly seen in Figure 9 that the clustering results of the traditional K-means algorithm contain many noise points and cannot obtain better clustering results. In Figure 10, K-means++ algorithm removes a lot of noise points. But there are many points with clustering errors, which cover up the edge information of the changing area and also cannot cluster the results. However, as shown in Figure 11, the change detection results obtained by this method can filter out the surrounding noise points well and retain the details of the change area, so the clustering results are more accurate. By comparing the results of the three clustering methods in Table 1, it can be seen that the improved K-means algorithm has the lowest error rate and the highest accuracy.

Table 1. Comparison of results of different algorithms.

Method	Detection rate	False detection rate	Accuracy
Traditional K-means	85.34%	25.26%	81.42%
K-means++	88.72%	24.35%	82.36%
Improved K-means	94.68%	9.41%	95.36%

Figure 12 is the optical map of the landslide site in the overall area monitored by the radar position. Figure 13 is the fusion image of radar data and unmanned aerial vehicle base map. The red and yellow areas are the deformation values of the landslide area. Combining the optical image with the radar monitoring and early warning image, it can be seen that the area detected in this paper is consistent with the actual landslide area. In practical applications, it can be used in combination with the radar monitoring and early warning information to provide quantitative analysis reference information. It ensures the life safety of production workers in the mining area and the safety of equipment and property.

Figure 12. Optical map of site after landslide.

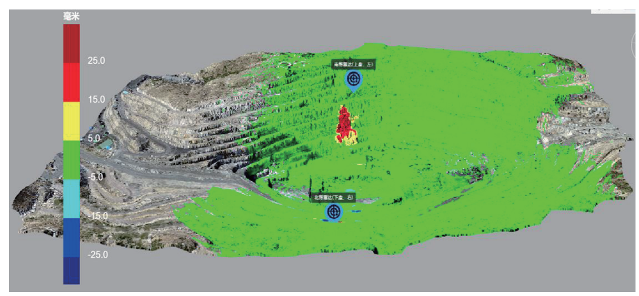

Figure 13. Early warning map of monitoring system.

4. CONCLUSION

For the micro-variation monitoring radar images with high spatial distortion and speckle noise, the coherence coefficient and logarithmic ratio cannot obtain a well-distinguished difference map. This paper combines the change characteristics of the coherence coefficient in the time series. First, the logarithmic ratio is calculated on the basis of the coherence coefficient, and then the difference map is obtained by the cumulative operation on the basis of the logarithmic ratio. It enhances the contrast between the changed area and unchanged area while suppressing a large amount of speckle noise, obtaining a better difference map. Additionally, the ability of wavelet multi-resolution analysis is used to further denoise the disparity map, making clustering easier. The improvement of the initial cluster center selection of k-means, adding the neighborhood decision term and fully combining the spatial and numerical information of the difference map. This makes it easier to find the most suitable cluster center position, reduce the number of iterations, and make the clustering result more stable and accurate.

By applying the proposed method to the measured data of the micro-variation monitoring radar, the improved results are compared with the traditional k-means algorithm for clustering effect. The result shows that the method in this paper is easier to find the center point of the cluster; the clustering effect is better; and the noise points are fewer. In the future, we will continue to explore the micro-variation monitoring radar image change detection algorithm to obtain more accurate change detection results.

ACKNOWLEDGMENT

This work was supported in part by Regional Programs of the National Natural Science Foundation of China under Grant 52064039, the General Project of Natural Science Foundation of Inner Mongolia Autonomous Region under Grant 2021MS06004 and the Fundamental scientific research projects of colleges and universities directly under the Inner Mongolia Autonomous Region under Grant JY20220174. The other part is supported by the Scientific research project of Inner Mongolia University of Technology under Grant DC2000001249 and the major science and technology special project of Inner Mongolia Autonomous Region 2019ZD022.

REFERENCES

1. Wang, Y., L. Du, and H. Dai, "Unsupervised SAR image change detection based on SIFT keypoints and region information," *IEEE Geoscience and Remote Sensing Letters*, Vol. 13, No. 7, 931–935, July 2016.
2. Ren, H., P. Huang, W. Tan, W. Xu, F. Liu, and M. Zhang, "Unsupervised image change detection based on ground-based imaging radar," *2019 IEEE International Conference on Signal, Information and Data Processing (ICSIDP)*, 1–5, 2019.
3. Zhuang, H. Fan, H. Deng, K. Yao, and B. Guo, "A spatial-temporal adaptive neighborhood-based ratio approach for change detection in SAR images," *Remote Sensing*, Vol. 10, No. 8, 2018.
4. Zhang, X., W. Liu, and S. He, "Urban change detection in TerraSAR image using the difference method and sar coherence coefficient," *Journal of Engineering Science And Technology Review*, Vol. 11, No. 3, 18–23, 2018.
5. Bovolo, F. and L. Bruzzone, "A detail-preserving scale-driven approach to change detection in multitemporal SAR images," *IEEE Transactions on Geoscience and Remote Sensing*, Vol. 43, No. 12, 2963–2972, Dec. 2005.
6. Sumaiya, M., N. Kumari, R. Shantha, and Selva, "Logarithmic mean-based thresholding for SAR image change detection," *IEEE Geoscience and Remote Sensing Letters*, Vol. 13, No. 11, 1726–1728, 2016.
7. Arai and Kohei, "Change detection method with multi-temporal satellite images based on wavelet decomposition and tiling," *International Journal of Modern Physics A*, Vol. 12, No. 3, 56–61, 2021.
8. Zhou, Y., L. Zhang, and P. Hua, "Combined simulated annealing and soft-threshold wavelet denoising of SAR image," *Journal of Beijing University of Aeronautics and Astronautics*, Vol. 32, No. 3, 293–296, 2006.
9. Yetgin, Z., "Unsupervised change detection of satellite images using local gradual descent," *IEEE Transactions on Geoscience and Remote Sensing*, Vol. 50, No. 5, 1919–1929, May 2012.
10. Liu, L., Z. Jia, J. Yang, and N. K. Kasabov, "SAR image change detection based on mathematical morphology and the K-means clustering algorithm," *IEEE Access*, Vol. 7, 43970–43978, 2019.